Supplementary Materials

Swine model and *in vivo* exposure to AVS risk factors

The study was conducted under a research protocol approved by the Institutional Animal Care and Use Committee through a Cooperative Research and Development Agreement (CRADA) between the University of Pennsylvania and the FDA. Ten mature castrated domestic male swine (~6 mo, 215 ± 36 lbs, Yorkshire cross Landrace) were randomly assigned to each of two diets for the two weeks prior to tissue collection: a standard corn/soybean diet (n=5) or a diet high in fat (12%) and cholesterol (1.5%) that was isocaloric to the standard diet (n=5). To assess the development of AVS, nine swine were fed the high-fat/high-cholesterol diet for 6 months and nine swine were maintained on a standard diet for 6 months. For tissue collection, the animals were placed under general anesthesia, anticoagulated and euthanized by exsanguination. The aortic valves were dissected immediately *post mortem* and processed as outlined below. Endothelium from the 2 wk HC valves were then processed for transcript profiling; tissue from both the 2 week and 6 month cohorts were processed for histology and IHC.

Swine lipid profiles

Blood samples were collected immediately prior to sacrificing the animals and excising the aortic valves. Following 2 weeks of a hypercholesterolemic diet (HC), swine developed hypercholesterolemia as shown by the blood lipid levels **(Suppl. Table S1).** Similarly, following 6 months of HC diet, swine had elevated blood lipid levels **(Suppl. Table S2).**

Group	Total Cholesterol (mg/dl)	HDL (mg/dl)	Triglycerides (mg/dl)
NC (N=5)	72.8 ± 6.1	29.2 ± 3.3	17.4 ± 4.2
HC (N=5)	549.2 ± 114.3	108.6 ± 16.4	7.8 ± 2.7

Supplementary Table S1: Serum lipid levels of male swine fed a normal (NC) or hypercholesterolemic (HC) diet for 2 weeks. Values are mean ± standard deviation.

Group	Total Cholesterol (mg/dl)	HDL (mg/dl)	Triglycerides (mg/dl)
NC (N=9)	60.0 ± 7.9	20.9 ± 4.1	8.4 ± 5.2
HC (N=9)	337.1 ± 51.0	86.1 ± 9.7	9.4 ± 10.8

Supplementary Table S2: Serum lipid levels of male swine fed a normal (NC) or hypercholesterolemic (HC) diet for 6 months. Values are mean ± standard deviation.

Sub-endothelial valve calcification in hypercholesterolemia

2 weeks HC: Occasional early calcific nodules were noted beneath the endothelium of the A side of some valve leaflets following 2 weeks hypercholesterolemia. Two examples are shown in Figure **S1a). Inset:** Alizarin crimson staining.

6 months HC: Significant calcific nodules were observed on the A-side in the mid regions of valve leaflets following 6 months hypercholesterolemia. These were apparent at gross dissection **(Figure S1b).**

Figure S1

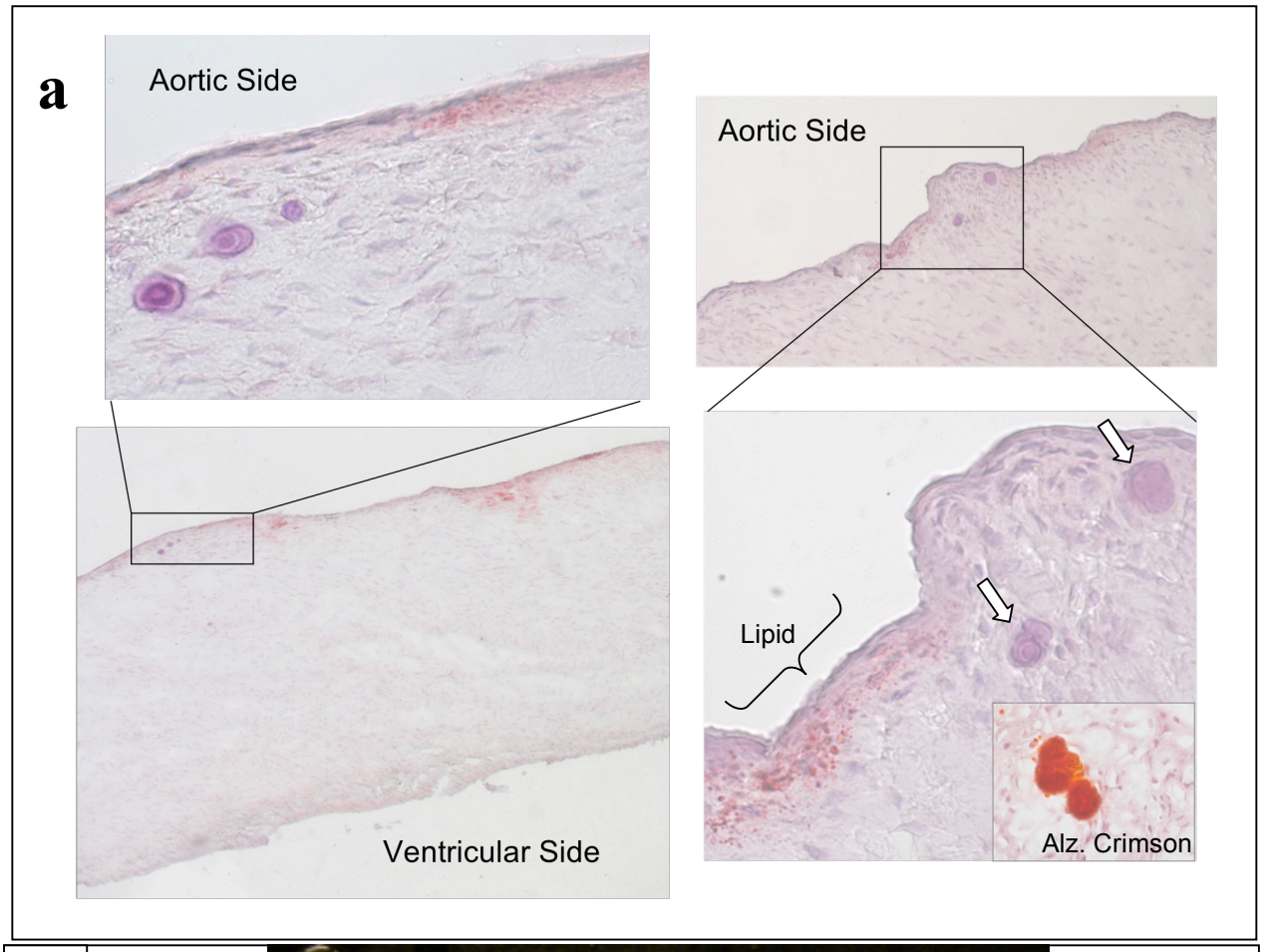
a
Aortic Side
Aortic Side
Ventricular Side
Lipid
Alz. Crimson
b

Staining for inflammatory markers

Frank inflammation was not seen even at 6 mo HC, therefore the distribution of ICAM and VCAM was assessed. These inflammatory mediators were irregularly expressed on both the A and V sides, and expression did not correlate with regions of lipid deposition (Figure S2). This is consistent with two previous studies which have shown variable ICAM and VCAM staining at sites of sclerotic lesions in human aortic valves.[1, 2]

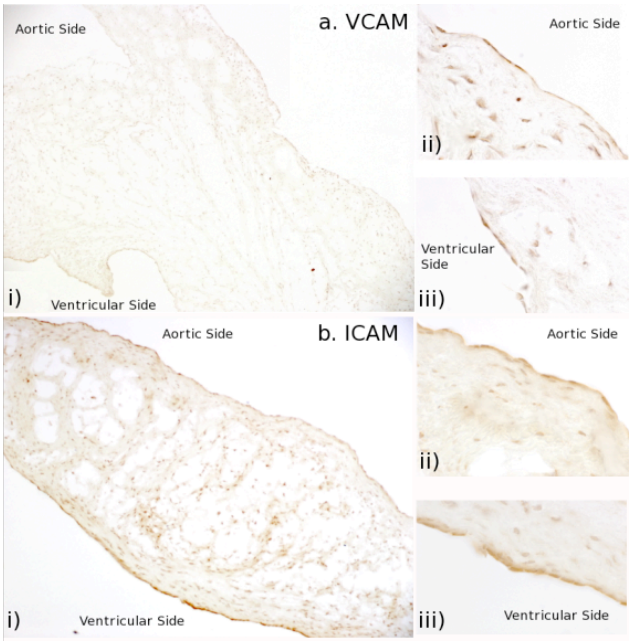

Figure S2: Immunocytochemical staining following 6 months hypercholesterolemia. **a.** Vascular Cell Adhesion Molecule (VCAM)-1. **b.** Intercellular Adhesion Molecule (ICAM)-1. Endothelial expression of each adhesion molecule was uneven on both sides of the valve leaflet.

EC Isolation and RNA processing (2 weeks groups only)

Endothelial cells were isolated from the A and V sides of aortic valve leaflets using a modified Haütchen method.[3] Briefly, each valve was flattened between 2 circular coverslips. A metal rod cooled to -20 ^{0}C in cold isopentane was applied directly to the top coverslip. The coverslips quickly froze onto the valve, adhering to the endothelial

cells which were then pulled from the leaflet. The cells from the A (or V) side of three leaflets for each valve were suspended in lysis buffer, pooled, and frozen on dry ice. The identity of cells isolated by this method has been confirmed by immunostaining for endothelial cell markers CD31 and von Willebrand factor and the absence of α-smooth muscle actin and CD45-positive leukocytes.[3]

RNA was isolated from the endothelial cells using a silica-based fiber matrix method (Absolutely RNA Nanoprep Kit, Stratagene) and assessed for quality using an Agilent Bioanalyzer 2100 (Agilent Technologies). A ratio of ~2:1 between 28S and 18S ribosomal RNA bands confirmed the integrity of the RNA. A range of 80-300ng of RNA was obtained per aortic valve side per animal. RNA underwent two rounds of linear amplification using T7-mediated *in vitro* transcription of mRNA, during which amino-allyl-UTP nucleotides are incorporated into aRNA.[4] The samples were indirectly labeled with Cy3 and Cy5 fluorescent dyes, fragmented to increase sensitivity, combined with hybridization buffer and herring sperm DNA, and hybridized onto porcine oligo microarrays overnight using a stepdown protocol (40 ^{0}C, 37 ^{0}C, 35 ^{0}C each for 5 hrs). The slides were washed with increasing stringency wash buffers, rinsed with post wash buffer, and dried by centrifugation.

Oligo microarrays were printed at the University of Pennsylvania Microarray Core Facility using Operon's Pig Array-Ready Oligo Set, which includes 70-mer probes for 10,665 genes from The Institute for Genomic Research porcine database; these included most annotated genes. The oligomers are designed to have minimal hairpin structure and cross-hybridization and are 3' biased to ensure adequate signal. Control spots and three

sets of custom oligos including additional genes known to play key roles in endothelial function were also printed onto the arrays.

Differential gene expression analysis

The microarrays were scanned (Agilent Technologies) and Agilent Feature Extraction Software was applied. The data were annotated to be MIAME compliant (www.mged.org) and loaded into the University of Pennsylvania public microarray data repository RAD.[5] The raw data were normalized using print-tip loess algorithm from the Bioconductor marray package for R.[6] Patterns of Gene Expression (PaGE) software,[7] which uses the False Discovery Rate (FDR) method, was used to identify statistically significant differentially expressed genes, as previously described.[8, 9] The FDR was set at 25% for all differential gene expression analyses, so that 75% the predicted genes are expected to be true positives. The results were corroborated with significance analysis of microarray.[10]

Pathway analysis

Ingenuity Pathway Analysis (IPA) Software (Ingenuity® Systems, www.ingenuity.com) compares the list of differentially expressed genes with a database of known genes, gene interactions, and pathways. This permits evaluation of the global effects of risk factor exposure on heterogeneous endothelial cell phenotypes. IPA generates networks of related genes by overlaying the list of differentially expressed genes onto the largest manually curated global molecular network. A score is assigned to each group of genes that form a network such that a high score corresponds to a low p-value and a low probability that those differentially expressed genes are unrelated.[11] IPA also uses the list of differentially expressed genes to identify over-represented functional categories, which are similar to Gene Ontology classifications, and over-represented canonical pathways, which are based on Kyoto Encyclopedia of Genes and Genomes (KEGG) ligand pathways as well as a thorough review of journal articles, review articles, and textbooks. The adjacent **Key** identifies the molecular caategories used in IPA pathway illustrations.

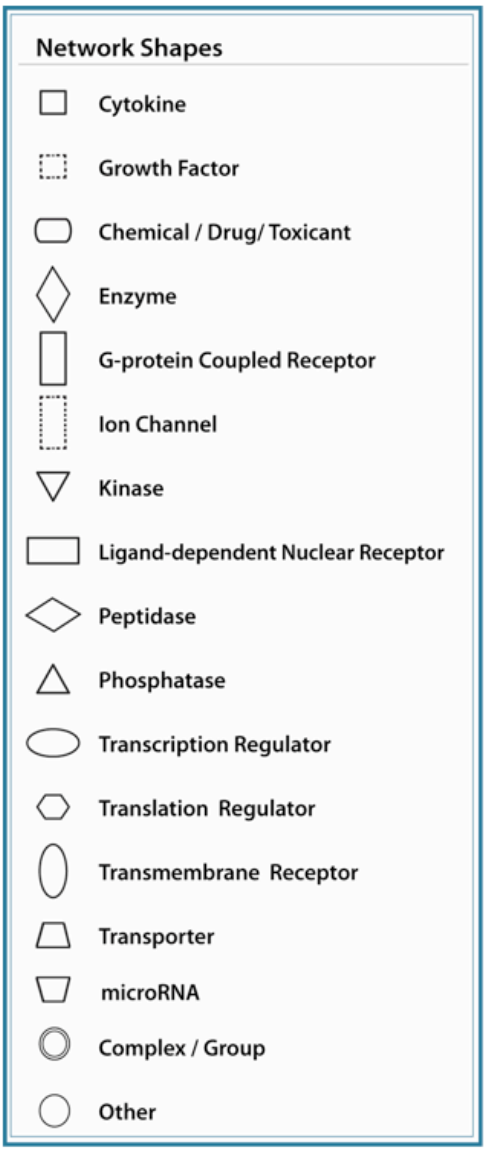

Key: Shapes that identify each molecular category in IPA Pathways Figures 2 and 3 of the main text.

Immunohistochemistry

Valve leaflet sections were fixed in 4% formaldehyde for 10 min and blocked with 3% H_2O_2 for 10 min and 10% horse serum for 30 min at 37 ^{0}C. Primary antibodies (PPARγ, L-FABP1, PRL, ABCA1 Santa Cruz Biotechnologies; HAM56, Novus Biologicals) were incubated overnight at 4 ^{0}C. After 20 min of PBS washes, secondary antibody (biotinylated anti-goat IgG and biotinylated anti-mouse IgG, Vector Labs) was applied for 1 hr. The sections were then incubated with Vector Labs ABC Reagent for 30 min, and the reaction was visualized with DAB.

Side-specific endothelial cell phenotypes in normocholesterolemia

A comparison between the aortic and ventricular side endothelial cells in normocholesterolemic animals identified 3013 genes differentially expressed (1479 up and 1534 down) on the A side relative to the V side. Specifically, the transcript profile of the A side relative to the V side revealed a pro-calcific endothelial phenotype, the absence of differential expression of key inflammatory mediators, such as intercellular adhesion molecule, vascular cell adhesion molecule, monocyte chemotactic protein 1, or tumor necrosis factor α (TNFα), and the downregulation of nuclear factor-κB (NF-κB) p65 subunit (RelA) on the A side, all consistent with an anti-inflammatory profile. **Supplementary Table S3** summarizes the pro-calcific gene expression differences prevalent in the A side endothelium.

Gene Name	A*vs*V	Consistent with (6)?
Osteoprotegerin (OPG, TNFRSF11b)	down	yes
Natriuretic peptide precursor C (NPPC)	down	yes
Chordin (CHRD)	down	yes
Parathyroid Hormone (PTH)	down	yes
Bone Morphogenic Protein 4 (BMP4)	up	yes
Pleiotrophin (PTN)	down	no
Hyaluronan and Proteoglycan Link Protein 1 (HAPLN)	up	yes
Osteocleast-stimulating Factor 1 (OSTF1)	up	yes

Supplementary Table S3: Pro-calcific endothelial phenotype expressed by aortic side endothelium in normocholesterolemia. Genes known to be protective for calcification (OPG, NPPC, CHRD, PTH, PTN) were downregulated on the aortic side while pro-calcific genes (BMP4, HAPLN, OSTF1) were upregulated. The final column confirms agreement with our previous study (1) of differential endothelial gene expression in the normal valve.

Pathway analyses of hypercholesterolemia-induced differential gene expression in aortic side endothelium

In addition to CASP3- and PPARγ-clusters discussed in the main text, several other gene pathways, including ANXA2- and TGFB1-clusters, were also differentially expressed in a manner consistent with a protective phenotype. For example, annexin A2 (ANXA2), which was downregulated by hypercholesterolemia, is a calcium-regulated phospholipid- and membrane-binding protein that may be involved in endosomal vesicular trafficking and responds to cholesterol in the endosome.[12] ANXA2 is also known to bind S100 calcium binding protein A10 (S100A10), forming a complex which may help organize membrane domains for early endosomes.[13] S100A10 may also function to localize ANXA2 to the cell surface in times of stress, creating a pro-coagulative environment.[14] The downregulation of these molecules is indicative of a protective response.

Transforming growth factor β1 (TGFβ1), although not differentially expressed, was closely linked to differentially expressed genes, including ANXA2, hairy/enhancer-of-split related with YRPW motif 1 (HEY1), prolactin (PRL), and TGFβ1-induced transcript 1 (TGFβI1). The expression pattern of these genes was consistent with decreased TGFβ1 signaling.[15-19] TGFβ1 is expressed in calcific and sclerotic valve leaflets and stimulates valvular interstitial cell calcification in vitro.[20] TGFβ1 is also known to decrease peroxisome proliferator-activated receptor γ (PPARγ) signaling both by decreasing human PPARγ mRNA[21] and by increasing phosphorylation of PPARγ protein.[22]

Gene expression in ventricular (V) side endothelium is largely uninfluenced by hypercholesterolemia

As noted in the manuscript in Table 1 and in contrast to the A side, few genes were differentially expressed on the V side in HC animals relative to normal animals. The only significant associations identified by IPA were for genes involved in G-protein signaling (Figure S3). Several genes for G-protein subunits and G-protein interacting peptides, which are known to be involved in such diverse endothelial cell processes as coagulation and solute sensing, were up-regulated on the V side of the valve in HC swine.

Gene Name
Inhibitory G protein, alpha subunit 1 (GNAI1)
Inhibitory G protein, alpha subunit 2 (GNAI2)
Activating G protein, alpha subunit O (GNAO1)
G protein, alpha subunit(G alpha)
Inhibitory G protein, alpha subunit (G alpha i)
Inhibitory G protein, alpha subunit O (Gai/o)

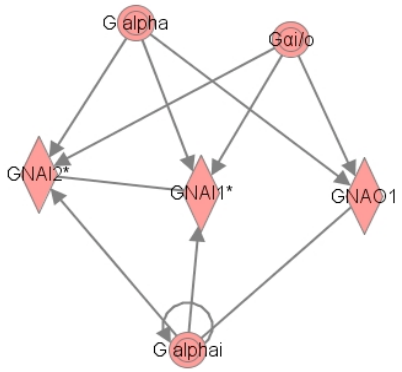

Figure S3: Few genes were differentially expressed on the V side endothelium in response to hypercholesterolemia. The only significant associations noted with pathway analysis were for genes involved in G-protein signaling.
Red and green represent genes up- and down-regulated, respectively, by HC relative to normocholesterolemia. The depth of color is proportional to the magnitude of differential expression. The shape of the gene box indicates the role of the gene product (see Key)

Paired A side to V side comparisons of endothelial gene expression in hypercholesterolemia corroborates a protective A side response

As outlined in the manuscript, the top scoring network from the *within* animal comparisons of A side endothelium to V side endothelium was TNF-centric and consistent with the downregulation of inflammatory mediators on the A side. For example, epoxidase (SQLE), which is the rate limiting enzyme in the synthesis of cholesterol from squalene,[23] was downregulated on the A side. Cholesterol has been shown to decrease SQLE transcript levels,[24] suggesting that the A side endothelium may be actively responding to hypercholesterolemia by downregulating cholesterol biosynthesis. Furthermore, TNF&[alpha] inhibitor protein 3 interacting protein 2 (TNIP2) was upregulated on the aortic side. TNIP2 binds A20, a potent inhibitor of NF&[kappa]B, to control NF&[kappa]B activation upstream of the NF&[kappa]B inhibitor kinase complex.[25]

Cytosolic phospholipase A2 (cPLA2), which is involved in the regulation of inflammation through the release of arachidonic acid from membrane phospholipids, was also upregulated on the A side. cPLA2 is subject to both transcriptional and post-translational regulation, the latter playing a key role in determining enzyme activity.[26] Three different cPLA2-activating pathways featured in the network were downregulated. Phospholipase A2-activating protein (PLAA) plays a direct role in controlling cPLA2.[27] Similarly, TNFα has been shown to increase cPLA2 activity both directly [28] and through an MAPKK1-ERK1/2 mediated pathway.[29] These findings suggest that though there may be increase in cPLA2 transcript level on the A side, the phenotype profile is consistent with a protective decrease in cPLA2 activation.

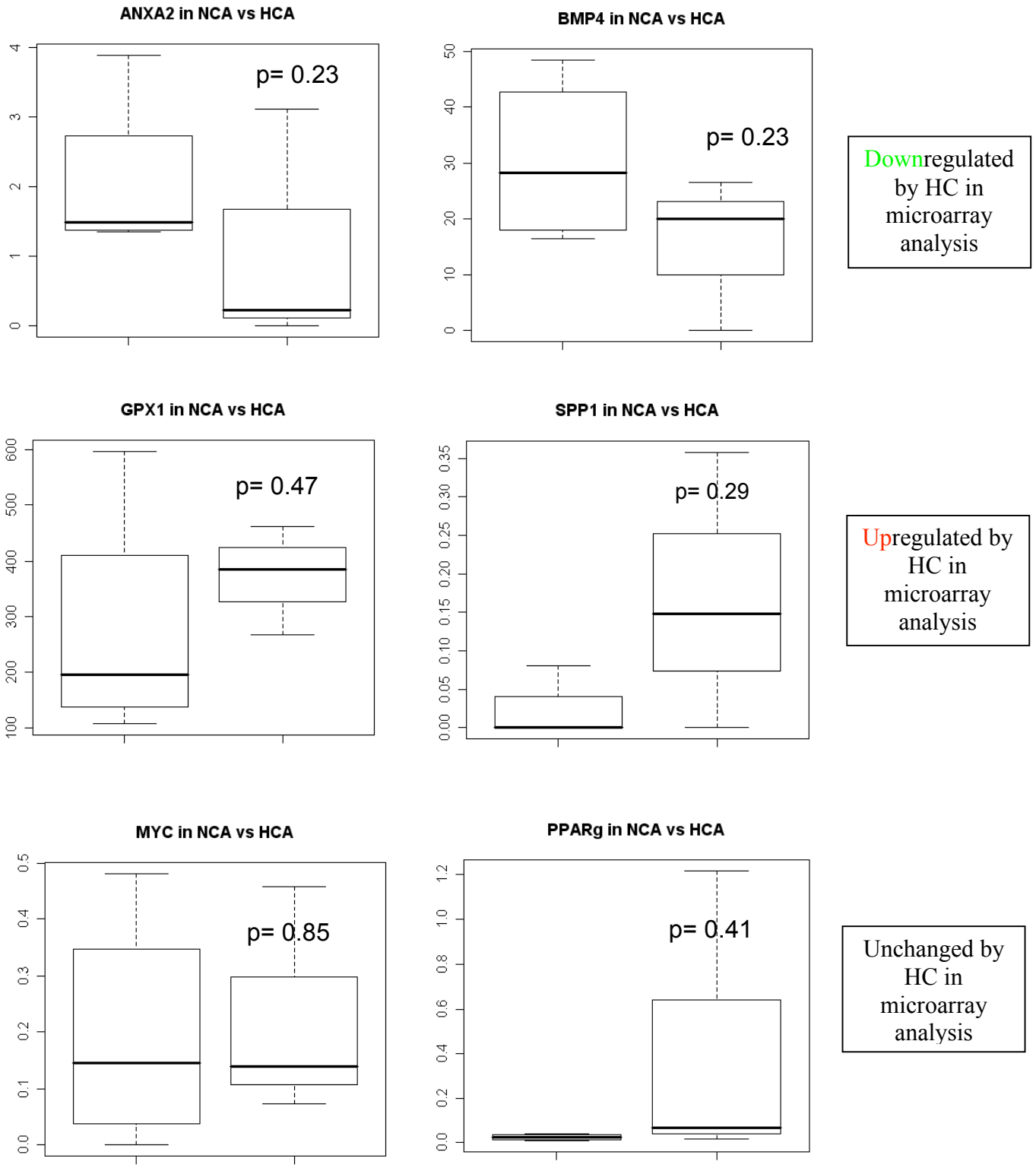

Supplementary Figure S2: The effect of hypercholesterolemia (HCA) vs normocholesterolemia (NCA) on A side expression of representative endothelial genes by QRT-PCR

Representative key genes downregulated, upregulated, or unchanged by microarray analyses were measured by QRT-PCR. Box plots illustrate the median value, the 25%-75% interquartile range, and the span of the data. NCA/HCA expression differences for ANXA2, BMP4, GPX1 and SPP1 (osteopontin) trended in the direction

identified by microarray but did not reach significance. PPARγ and MYC, which were not found to be differentially expressed at the gene level, showed no differences in the median expression

References:

1. Ghaisas NK, Foley JB, O'Briain DS, Crean P, Kelleher D, Walsh M. Adhesion molecules in nonrheumatic aortic valve disease: endothelial expression, serum levels and effects of valve replacement. *J Am Coll Cardiol.* 2000;36:2257-2262.
2. Muller AM, Cronen C, Kupferwasser LI, Oelert H, Muller KM, Kirkpatrick CJ. Expression of endothelial cell adhesion molecules on heart valves: up-regulation in degeneration as well as acute endocarditis. *J Pathol.* 2000;191:54-60.
3. Simmons CA, Zilberberg J, Davies PF. A rapid, reliable method to isolate high quality endothelial RNA from small spatially-defined locations. *Ann Biomed Eng.* 2004;32:1453-1459.
4. Van Gelder RN, von Zastrow ME, Yool A, Dement WC, Barchas JD, Eberwine JH. Amplified RNA synthesized from limited quantities of heterogeneous cDNA. *Proc Natl Acad Sci U S A.* 1990;87:1663-1667.
5. Manduchi E, Grant GR, He H, Liu J, Mailman MD, Pizarro AD, Whetzel PL, Stoeckert CJ, Jr. RAD and the RAD Study-Annotator: an approach to collection, organization and exchange of all relevant information for high-throughput gene expression studies. *Bioinformatics.* 2004;20:452-459.
6. Yang YH, Dudoit S, Luu P, Lin DM, Peng V, Ngai J, Speed TP. Normalization for cDNA microarray data: a robust composite method addressing single and multiple slide systematic variation. *Nucleic Acids Res.* 2002;30:e15.
7. Grant GR, Liu J, Stoeckert CJ, Jr. A practical false discovery rate approach to identifying patterns of differential expression in microarray data. *Bioinformatics.* 2005;21:2684-2690.
8. Simmons CA, Grant GR, Manduchi E, Davies PF. Spatial heterogeneity of endothelial phenotypes correlates with side-specific vulnerability to calcification in normal porcine aortic valves. *Circ Res.* 2005;96:792-799.
9. Passerini AG, Shi C, Francesco NM, Chuan P, Manduchi E, Grant GR, Stoeckert CJ, Jr., Karanian JW, Wray-Cahen D, Pritchard WF, Davies PF. Regional determinants of arterial endothelial phenotype dominate the impact of gender or short-term exposure to a high-fat diet. *Biochem Biophys Res Commun.* 2005;332:142-148.
10. Tusher VG, Tibshirani R, Chu G. Significance analysis of microarrays applied to the ionizing radiation response. *Proc Natl Acad Sci U S A.* 2001;98:5116-5121.
11. Calvano SE, Xiao W, Richards DR, Felciano RM, Baker HV, Cho RJ, Chen RO, Brownstein BH, Cobb JP, Tschoeke SK, Miller-Graziano C, Moldawer LL, Mindrinos MN, Davis RW, Tompkins RG, Lowry SF. A network-based analysis of systemic inflammation in humans. *Nature.* 2005;437:1032-1037.
12. Mayran N, Parton RG, Gruenberg J. Annexin II regulates multivesicular endosome biogenesis in the degradation pathway of animal cells. *EMBO J.* 2003;22:3242-3253.

13. Rety S, Sopkova J, Renouard M, Osterloh D, Gerke V, Tabaries S, Russo-Marie F, Lewit-Bentley A. The crystal structure of a complex of p11 with the annexin II N-terminal peptide. *Nat Struct Biol.* 1999;6:89-95.
14. Deora AB, Kreitzer G, Jacovina AT, Hajjar KA. An annexin 2 phosphorylation switch mediates p11-dependent translocation of annexin 2 to the cell surface. *J Biol Chem.* 2004;279:43411-43418.
15. Chambers RC, Leoni P, Kaminski N, Laurent GJ, Heller RA. Global expression profiling of fibroblast responses to transforming growth factor-beta1 reveals the induction of inhibitor of differentiation-1 and provides evidence of smooth muscle cell phenotypic switching. *Am J Pathol.* 2003;162:533-546.
16. Jikihara H, Handwerger S. Tumor necrosis factor-alpha inhibits the synthesis and release of human decidual prolactin. *Endocrinology.* 1994;134:353-357.
17. Shibanuma M, Mashimo J, Kuroki T, Nose K. Characterization of the TGF beta 1-inducible hic-5 gene that encodes a putative novel zinc finger protein and its possible involvement in cellular senescence. *J Biol Chem.* 1994;269:26767-26774.
18. Tan SK, Wang FF, Pu HF, Liu TC. Differential effect of age on transforming growth factor-beta 1 inhibition of prolactin gene expression versus secretion in rat anterior pituitary cells. *Endocrinology.* 1997;138:878-885.
19. Zavadil J, Cermak L, Soto-Nieves N, Bottinger EP. Integration of TGF-beta/Smad and Jagged1/Notch signalling in epithelial-to-mesenchymal transition. *EMBO J.* 2004;23:1155-1165.
20. Jian B, Narula N, Li QY, Mohler ER, 3rd, Levy RJ. Progression of aortic valve stenosis: TGF-beta1 is present in calcified aortic valve cusps and promotes aortic valve interstitial cell calcification via apoptosis. *Ann Thorac Surg.* 2003;75:457-465; discussion 465-456.
21. Zhou S, Lechpammer S, Greenberger JS, Glowacki J. Hypoxia inhibition of adipocytogenesis in human bone marrow stromal cells requires transforming growth factor-beta/Smad3 signaling. *J Biol Chem.* 2005;280:22688-22696.
22. Han J, Hajjar DP, Tauras JM, Feng J, Gotto AM, Jr., Nicholson AC. Transforming growth factor-beta1 (TGF-beta1) and TGF-beta2 decrease expression of CD36, the type B scavenger receptor, through mitogen-activated protein kinase phosphorylation of peroxisome proliferator-activated receptor-gamma. *J Biol Chem.* 2000;275:1241-1246.
23. Satoh T, Hidaka Y, Kamei T. Regulation of squalene epoxidase activity in rat liver. *J Lipid Res.* 1990;31:2095-2101.
24. Maxwell KN, Soccio RE, Duncan EM, Sehayek E, Breslow JL. Novel putative SREBP and LXR target genes identified by microarray analysis in liver of cholesterol-fed mice. *J Lipid Res.* 2003;44:2109-2119.
25. Van Huffel S, Delaei F, Heyninck K, De Valck D, Beyaert R. Identification of a novel A20-binding inhibitor of nuclear factor-kappa B activation termed ABIN-2. *J Biol Chem.* 2001;276:30216-30223.
26. Leslie CC. Properties and regulation of cytosolic phospholipase A2. *J Biol Chem.* 1997;272:16709-16712.

27. Ribardo DA, Crowe SE, Kuhl KR, Peterson JW, Chopra AK. Prostaglandin levels in stimulated macrophages are controlled by phospholipase A2-activating protein and by activation of phospholipase C and D. *J Biol Chem.* 2001;276:5467-5475.
28. Hoeck WG, Ramesha CS, Chang DJ, Fan N, Heller RA. Cytoplasmic phospholipase A2 activity and gene expression are stimulated by tumor necrosis factor: dexamethasone blocks the induced synthesis. *Proc Natl Acad Sci U S A.* 1993;90:4475-4479.
29. Pearce MJ, McIntyre TM, Prescott SM, Zimmerman GA, Whatley RE. Shear stress activates cytosolic phospholipase A2 (cPLA2) and MAP kinase in human endothelial cells. *Biochem Biophys Res Commun.* 1996;218:500-504.